

ECOLOGY

Global patterns and drivers of ecosystem functioning in rivers and riparian zones

Scott D. Tiegs*, David M. Costello, Mark W. Isken, Guy Woodward, Peter B. McIntyre, Mark O. Gessner, Eric Chauvet, Natalie A. Griffiths, Alex S. Flecker, Vicens Acuña, Ricardo Albariño, Daniel C. Allen, Cecilia Alonso, Patricio Andino, Clay Arango, Jukka Aroviita, Marcus V. M. Barbosa, Leon A. Barmuta, Colden V. Baxter, Thomas D. C. Bell, Brent Bellinger, Luz Boyero, Lee E. Brown, Andreas Bruder, Denise A. Bruesewitz, Francis J. Burdon, Marcos Callisto, Cristina Canhoto, Krista A. Capps, María M. Castillo, Joanne Clapcott, Fanny Colas, Checo Colón-Gaud, Julien Cornut, Verónica Crespo-Pérez, Wyatt F. Cross, Joseph M. Culp, Michael Danger, Olivier Dangles, Elvira de Eyto, Alison M. Derry, Veronica Díaz Villanueva, Michael M. Douglas, Arturo Elosegí, Andrea C. Encalada, Sally Entekin, Rodrigo Espinosa, Diana Ethaiya, Verónica Ferreira, Carmen Ferriol, Kyla M. Flanagan, Tadeusz Fleituch, Jennifer J. Follstad Shah, André Frainer, Nikolai Friberg, Paul C. Frost, Erica A. Garcia, Liliana García Lago, Pavel Ernesto García Soto, Sudeep Ghate, Darren P. Giling, Alan Gilmer, José Francisco Gonçalves Jr., Rosario Karina Gonzales, Manuel A. S. Graça, Mike Grace, Hans-Peter Grossart, François Guérol, Vlad Gulis, Luiz U. Hepp, Scott Higgins, Takuo Hishi, Joseph Huddart, John Hudson, Samantha Imberger, Carlos Iñiguez-Armijos, Tomoya Iwata, David J. Janetski, Eleanor Jennings, Andrea E. Kirkwood, Aaron A. Koning, Sarian Kosten, Kevin A. Kuehn, Hjalmar Laudon, Peter R. Leavitt, Aurea L. Lemes da Silva, Shawn J. Leroux, Carri J. LeRoy, Peter J. Lisi, Richard MacKenzie, Amy M. Marcarelli, Frank O. Masese, Brendan G. McKie, Adriana Oliveira Medeiros, Kristian Meissner, Marko Miliša, Shailendra Mishra, Yo Miyake, Ashley Moerke, Shorok Mombrikotb, Rob Mooney, Tim Moulton, Timo Muotka, Junjiro N. Negishi, Vinicius Neres-Lima, Mika L. Nieminen, Jorge Nimptsch, Jakub Ondruch, Riku Paavola, Isabel Pardo, Christopher J. Patrick, Edwin T. H. M. Peeters, Jesus Pozo, Catherine Pringle, Aaron Prussian, Estefania Quenta, Antonio Quesada, Brian Reid, John S. Richardson, Anna Rigosi, José Rincón, Geta Rîsnoveanu, Christopher T. Robinson, Lorena Rodríguez-Gallego, Todd V. Royer, James A. Rusak, Anna C. Santamans, Géza B. Selmeçy, Gelas Simiyu, Agnija Skuja, Jerzy Smykla, Kandikere R. Sridhar, Ryan Sponseller, Aaron Stoler, Christopher M. Swan, David Szlag, Franco Teixeira-de Mello, Jonathan D. Tonkin, Sari Uusheimo, Allison M. Veach, Sirje Vilbaste, Lena B. M. Vought, Chiao-Ping Wang, Jackson R. Webster, Paul B. Wilson, Stefan Woelfl, Marguerite A. Xenopoulos, Adam G. Yates, Chihiro Yoshimura, Catherine M. Yule, Yixin X. Zhang, Jacob A. Zwart†

River ecosystems receive and process vast quantities of terrestrial organic carbon, the fate of which depends strongly on microbial activity. Variation in and controls of processing rates, however, are poorly characterized at the global scale. In response, we used a peer-sourced research network and a highly standardized carbon processing assay to conduct a global-scale field experiment in greater than 1000 river and riparian sites. We found that Earth's biomes have distinct carbon processing signatures. Slow processing is evident across latitudes, whereas rapid rates are restricted to lower latitudes. Both the mean rate and variability decline with latitude, suggesting temperature constraints toward the poles and greater roles for other environmental drivers (e.g., nutrient loading) toward the equator. These results and data set the stage for unprecedented "next-generation biomonitoring" by establishing baselines to help quantify environmental impacts to the functioning of ecosystems at a global scale.

INTRODUCTION

Organic carbon that enters river and riparian ecosystems meets one of many fates: It is mineralized and released to the atmosphere as CO₂ or CH₄, incorporated into local food webs, or routed downstream to

join long-term storage pools in marine or lake sediments (1–3). The rate at which organic carbon is processed determines which of these fates predominates and has important implications for the functioning of ecosystems from local to global scales. While rates vary widely over broad spatial scales (4, 5), logistical constraints and standardization issues have hindered elucidation of global patterns and environmental controls. Many investigations have explored organic-matter processing

Copyright © 2019
The Authors, some
rights reserved;
exclusive licensee
American Association
for the Advancement
of Science. No claim to
original U.S. Government
Works. Distributed
under a Creative
Commons Attribution
NonCommercial
License 4.0 (CC BY-NC).

Downloaded from <https://www.science.org> at Texas A&M University, Corpus Christi on October 10, 2022

*Corresponding author. Email: tiegs@oakland.edu

†Author affiliations noted in Supplementary Materials.

in streams and rivers (fig. S1), but methodological differences among studies—especially the use of different substrates—have impeded mechanistic understanding of what drives carbon processing rates at large spatial scales. For example, the quality of leaf litter used in decomposition assays varies systematically across the planet, potentially masking patterns in carbon processing attributable to extrinsic factors such as microbial community structure and environmental conditions—factors that are increasingly affected by human activities. Because different substrates are used across studies, we have an underdeveloped knowledge of the degree to which rates are controlled by substrate quality or by the microbial communities and environmental conditions that characterize a particular location. Overcoming these methodological limitations and filling these knowledge gaps is necessary to gauge large-scale controls on carbon processing, establish baselines for emerging global assessment initiatives (e.g., Intergovernmental Science-Policy Platform on Biodiversity and Ecosystem Services and Intergovernmental Panel on Climate Change), and accurately quantify human impacts to the global carbon cycle (6–8).

To these ends, we report findings from the first global Cellulose Decomposition Experiment (CELDEX), which combines a rigorously

standardized bioassay with a peer-sourced network of research professionals to evaluate carbon processing rates in Earth's rivers and riparian zones. We applied a standardized cotton-strip assay (9, 10) simultaneously in river channels and adjacent riparian habitats to quantify microbial decomposition of cellulose, the most abundant polymer on Earth, the main component of terrestrial plant litter, and an important source of greenhouse gas emissions from riverine ecosystems (11). This assay quantifies the inherent capacity of ecosystems to process organic carbon—their decomposition potential—and integrates the influences of microbial community structure and environmental factors such as nutrient availability, temperature, and moisture on microbial activity. A key advantage of the assay is that it lacks variation in substrate attributes such as nutrient content and toughness. Experimental materials were distributed to 150 researchers in the CELDEX Consortium from ~125 institutions who deployed and retrieved the strips at more than 1000 river and riparian sites. Cotton strips were then returned to the coordinating laboratory for standardized measurements of the degree of decomposition. Field sites spanned 140° of latitude, were located on all continents, and included each of Earth's major biomes (Fig. 1A). Because we used an identical assay across all sites,

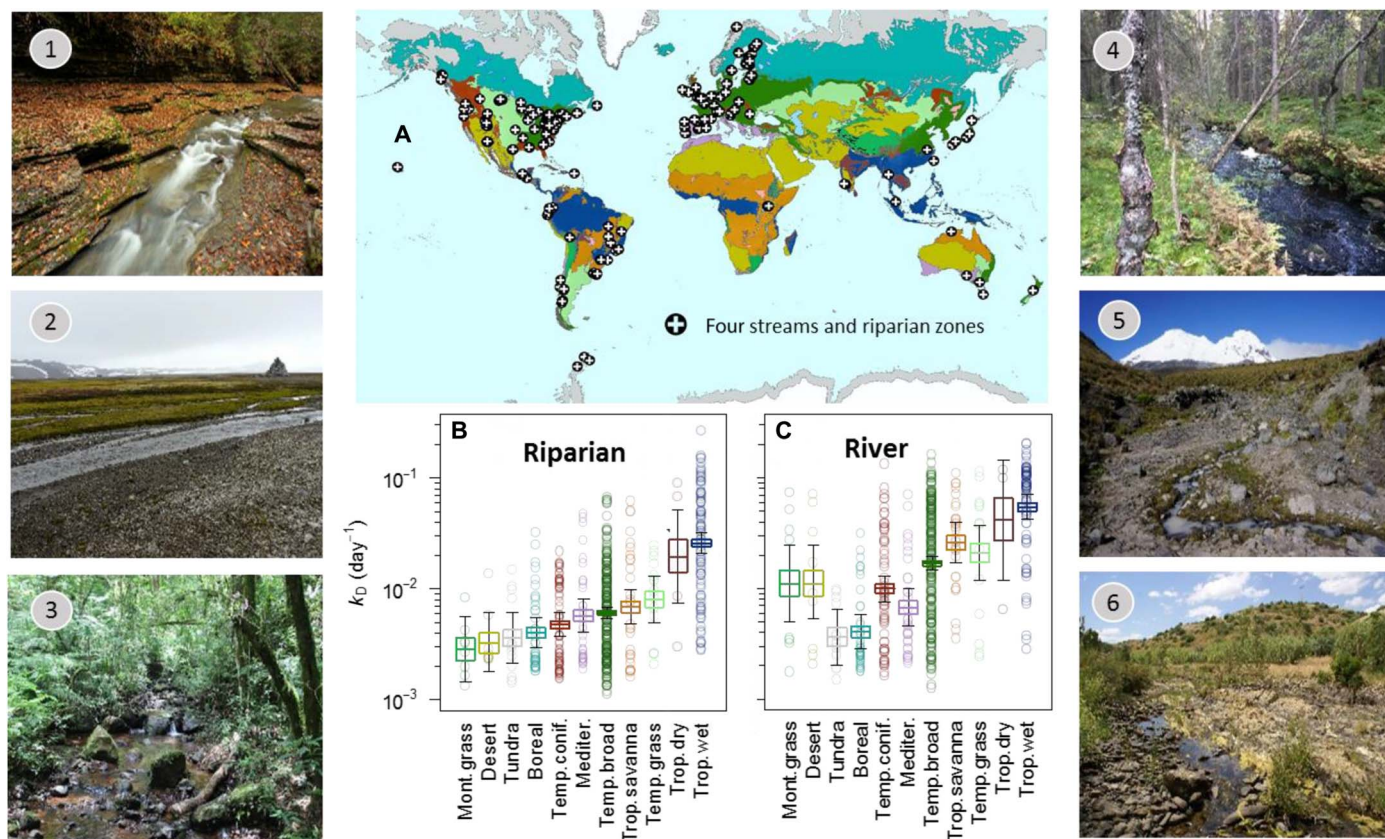


Fig. 1. Global distribution of field sites, mean decomposition rates across biomes, and photos of select field sites. More than 500 river-riparian pairs ($n = 514$ river, $n = 533$ riparian) were located in approximately 40 countries, on each continent, and spanned more than 140° of latitude. Colors correspond to Earth's major terrestrial biomes (A). The estimated mean decomposition rates ($\pm 95\%$ credible intervals) of cotton strips (k_D) varied across biomes in riparian zones (B) and their adjacent rivers (C). Photographs are shown for rivers and zones in temperate broadleaf forests (1), tundra (2), tropical wet forests (3), boreal forests (4), montane grassland (5), and Mediterranean ecosystems (6). Photo credits: Stream 1. Olivier Dangles, Centre d'Ecologie Fonctionnelle et Evolutive, IRD, CNRS. Stream 2. Jerzy Smykla, Institute of Nature Conservation, Polish Academy of Sciences. Stream 3. Luis Hepp, Department of Biological Sciences, Regional Integrated University of Upper Uruguay and Missions. Stream 4. Jukka Aroviita, Finnish Environment Institute (SYKE). Stream 5. Scott Tiegs, Department of Biological Sciences, Oakland University. Stream 6. Manuel Graça, MARE—Marine and Environmental Sciences Centre, University of Coimbra.

we were also able to relate the wide-ranging processing rates that we observed to large-scale environmental drivers of carbon processing in a biogeographical and climatic context.

RESULTS AND DISCUSSION

We found that Earth's major biomes have distinct carbon processing signatures in both rivers and riparian zones (Fig. 1). Rates are lowest in cold biomes, such as tundra and boreal forests, whereas those in tropical forests (both wet and dry) are up to an order of magnitude greater; most temperate biomes are bracketed by these extremes (Fig. 1, B and C). These patterns suggest that—similar to terrestrial ecosystems—broad-scale climatic factors, temperature and precipitation, are master variables that set the boundaries of carbon processing rates in rivers and riparian zones at the global scale. Biome identity accounted for a similar amount of variance in rivers and riparian habitats (30% versus 28%, respectively); this similarity is notable because the biome concept was originally developed for terrestrial rather than aquatic ecosystems (12). This highlights the close coupling between riverine ecosystems, their catchments and regional climate, and the utility of the biome concept for river and riparian ecosystems.

Knowledge of ecosystem functioning in tropical rivers and riparian zones is poorly developed, even though these rivers constitute >50% of Earth's runoff (12) and form a major carbon input to the global ocean (13). Moreover, tropical rivers are hot spots for CO₂ evasion (14, 15), yet whether the predominant source is instream decomposition of organic matter (dissolved and particulate) derived from terrestrial plants, or CO₂ imported from terrestrial root and soil respiration (14), is largely unknown. Very high terrestrial primary production in tropical forests generates vast quantities of plant litter, and our data show that cellulose—

the most abundant litter constituent—can be very effectively processed by microbial communities in tropical rivers and riparian areas (Fig. 1, B and C). This rapid processing occurred despite the fact that the cellulose substrate does not supply substantial amounts of nutrients (e.g., nitrogen and phosphorus) to facilitate decomposition. Although the cellulose used in our assay differed in quality from the litter that enters tropical rivers, the exceptionally rapid decomposition that we observed is a novel line of evidence suggesting that the microbial processing of plant material is a major CO₂ source (11, 14, 15).

We found clear patterns of processing rates with latitude; both the upper limit of processing rates and variability among rivers and riparian zones decrease with latitude (Fig. 2, A and B). These results are evidenced by the increasing slope of each quantile in these relationships (Fig. 2, A and B, insets), revealing that carbon processing can be slow anywhere on the planet, whereas rapid rates are reached only at low latitudes. Dampening of peak rates with distance from the equator suggests tighter climatic constraints toward the poles—such as temperature limitation—and that additional factors (e.g., nutrient availability, pH, and microbial-community structure) come into play toward the equator.

Across a broad range of quantiles, the slope of relationships between processing rates and latitude is greater in rivers compared to riparian zones, a finding that suggests that rivers are more sensitive to parameters that covary with latitude (e.g., temperature) (Fig. 2, A and B, insets). For sites with the slowest decomposition rates (i.e., quantiles 5 to 10%), the lack of a slope illustrates that slow rates can be found across the broad range of latitudes that we examined, in both rivers and riparian zones. For the majority of the data (quantiles 15 to 80%), the slope of the relationship between rates and latitude is greater in rivers, evidenced by nonoverlapping credible intervals between

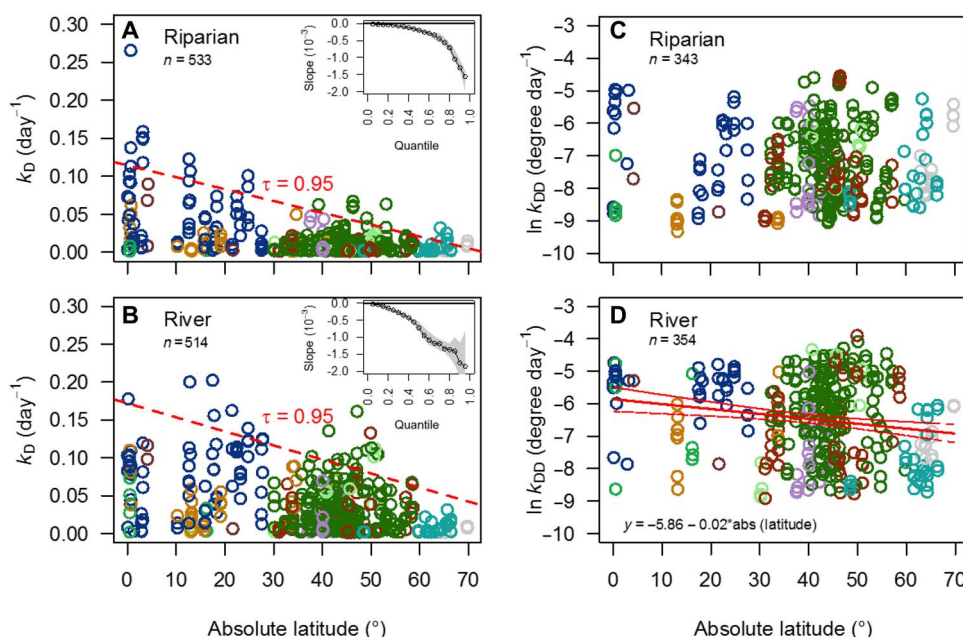


Fig. 2. Relationships between absolute latitude and decomposition rates in riparian zones and rivers. Quantile regression in riparian zones (A) and rivers (B) showing decomposition rates per day (k_D) versus latitude and the 95th quantile (dashed line). Inset panels (A) and (B) show the increasing slope of regression lines with each 5-centile. In each habitat, slow decomposition can be observed regardless of latitude; latitude, however, imposes a strong upper constraint on decay rates. When the effect of temperature is removed by expressing decomposition on a per-degree-day basis (k_{DD}) (C and D), there is no significant relationship between decomposition and latitude in riparian zones (C), and a negative relationship is observed with latitude in rivers (D). Colors match the biomes shown in Fig. 1.

these two habitat types; this greater slope indicates that decomposition in rivers is more sensitive to changes in latitude. For ecosystems that decompose the fastest (i.e., quantiles >85%), the variability among rivers is large and our estimate of the relationships with latitude is not well constrained and is therefore not significantly different between rivers and riparian zones.

In an extensive meta-analysis of data on leaf-litter processing, rates of microbial processing in rivers increased with latitude even after accounting for strong covariation of temperature (5). The proposed mechanism for the increase was physiological adaptation that enables river microbes to remain active during periods of peak litter inputs despite low temperatures. However, our data show that when a standard substrate is used to control for variation in litter quality, temperature-normalized processing rates in rivers decline with latitude (Fig. 2D), with the normalized rates, on average, being 4.1 times greater near the equator than at our highest latitude sites. No relationship was observed in riparian zones (Fig. 2C), suggesting that in these habitats, the environmental variables that covary with latitude are of secondary importance to others, such as moisture limitation as a prime factor. In rivers and riparian zones, we documented considerable variation in temperature-normalized rates across most latitudes, highlighting the variety of environmental conditions that influenced decomposition rates, and the need for additional information beyond geographic location to explain them.

Differences in litter substrate choice are a plausible explanation for contrasting results between our study—which made use of a single standard substrate—and the global meta-analysis—which synthesized studies across many locally collected types of leaf litter. Plant traits vary systematically across large spatial scales (16, 17), as does the quality of riparian leaves and litter (18), both of which increase with latitude. For example, the phosphorus content of leaves increases with distance from the equator (18), a pattern that could foster large-scale adaptations that enable stream microbes to decompose substrates of poor nutrient content, such as litter rich in cellulose and lignin. Together with previous results, ours suggest that, independently of temperature, the inherent capacity of ecosystems to decompose organic matter declines with latitude but that systematic global variation in litter traits might mask these effects and cause apparent decomposition rates to increase with latitude. This highlights the necessity for a standard substrate when using decomposition assays as part of large-scale bioassessment protocols.

Rivers and their riparian zones are closely connected through reciprocal exchanges of organic carbon, and processes in one habitat have ramifications for the other (19, 20). To better understand their relative functioning, we evaluated the log ratio of carbon processing rates in paired river-riparian sites. We found that rivers have rates (k_D) that are, on average, nearly twice those of the adjacent riparian habitats (median River k_D /Riparian k_D = 1.77, n = 514 sites) (Fig. 3). Standardizing for temperature (k_{DD}) does not change the magnitude of this disparity (median River k_{DD} /Riparian k_{DD} = 1.86, n = 314 sites), reflecting the strong correlation between average air and water temperature. The ratio varies widely across sites, ranging from 70 to 0.05 (fig. S2). Rates in riparian zones of montane grasslands and deserts are extremely slow (Fig. 1B), whereas rates in the adjacent river channels are similar to the global average (Figs. 1C and 3). In contrast, cellulose-decomposition rates in only 2.5% of riparian zones significantly exceeded those in rivers (fig. S2). Given the exchange of carbon between rivers and riparian zones, and their discrepancy in processing potentials between these two habitats, streams are hot spots for carbon processing, while riparian

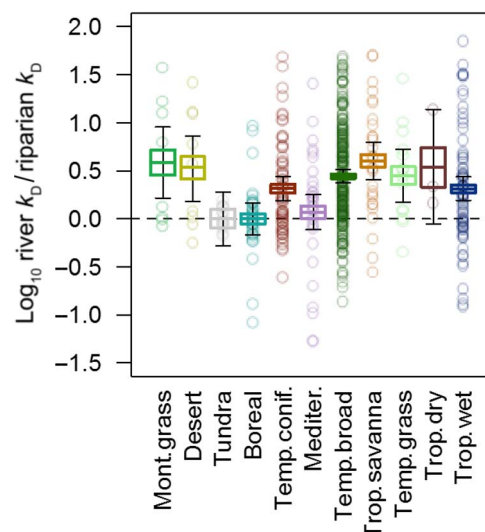


Fig. 3. The log response ratio of river decomposition (k_D) to riparian decomposition (k_D). Bayesian estimates of median ratios are shown as horizontal lines, with 50 and 95% credible intervals of the median as the box and whiskers, respectively. Open symbols show individual riparian-river pairs color-coded by biome (n = 514). Values greater than zero (dashed line) indicate significantly more rapid decomposition in rivers relative to their riparian zones.

zones, given their relatively slow carbon turnover, likely serve as sources of organic carbon well past periods of organic matter input (e.g., autumn leaf fall in temperate zones). The magnitude of river/riparian processing rates shows no relationship with latitude (fig. S3A), unless the effects of temperature are removed and then a negative relationship emerges (fig. S3B). This finding indicates that the relative difference in temperature-adjusted processing between habitats is, on average, greater toward the poles. Variation in the relative processing rates of rivers and riparian zones highlights functional biodiversity across broad latitudinal gradients and across Earth's biomes. And in many biomes this variation highlights the importance of local habitat diversity to create heterogeneity in ecosystem functioning at a landscape scale.

The variable relative processing rates in coupled riparian-river habitats may be caused by differential temperature sensitivity between rivers and riparian zones. The significantly greater apparent activation energy calculated for river channels (0.68 eV) shows that, on average, carbon processing in river habitats is far more sensitive to temperature than in riparian zones (0.40 eV; Fig. 4). This terrestrial-aquatic disparity mirrors patterns in a meta-analysis of whole-ecosystem respiration (21) and our river data almost exactly match the theoretically expected activation energy according to the metabolic theory of ecology (22). These disparities suggest that different drivers are at play in river channels and riparian habitats, with water limitation being an obvious contender. This moisture-limitation hypothesis is further supported by similar decomposition rates observed in riparian and river habitats of cool mesic biomes, such as tundra and boreal forests (Fig. 3).

Because different factors constrain carbon processing in riparian and river habitats, responses to environmental change could differ greatly among biomes and habitats. In particular, warming and aridity are both predicted to increase across vast areas of the planet (23), a climatic trend that should increase processing rates in rivers

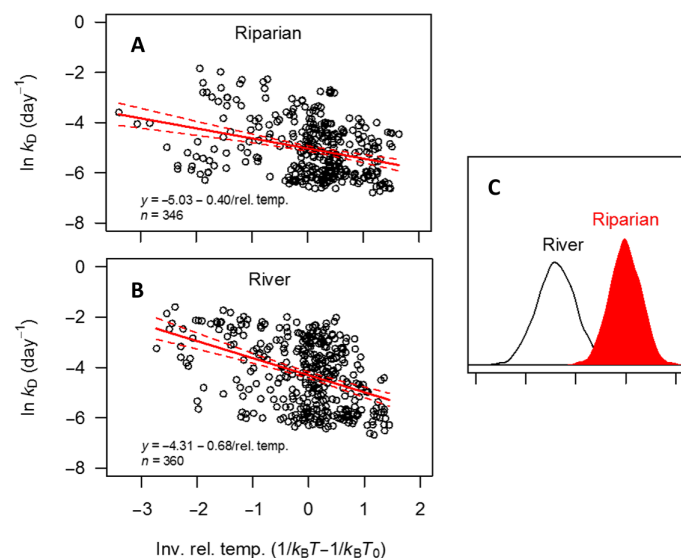


Fig. 4. Temperature sensitivity of cellulose decomposition in riparian zones and rivers. Arrhenius plots illustrating differences in the apparent activation energies of decomposition in riparian zones (A), 0.40 eV and rivers (B), 0.68 eV. (C) Posterior distribution of the slope estimates (i.e., apparent activation energy estimates), indicating that neither of the slopes overlap with zero (i.e., they are statistically significant) and that there is very little overlap between the slope estimates for decomposition in rivers and riparian zones.

yet decrease them in riparian zones. This dimension of relative processing rates between rivers and riparian zones—differential responses of a process between habitats under environmental change—represents a yet-to-be-explored portfolio effect (24) arising from habitat diversity that stabilizes mean processing rates at the landscape scale.

CONCLUSIONS

The >1000 river and riparian sites used in our study were deemed relatively free of human impacts. Consequently, by using an identical assay at all sites, we can unambiguously ascribe the variability that we document to naturally variable environmental conditions and biotic communities. Importantly, these environmental drivers include those that are increasingly affected by human activities such as temperature and moisture availability. This sensitivity to anthropogenically affected variables gives our data added value as a baseline for the biomonitoring of a functional ecosystem property. Moreover, the validated utility of combining a straightforward field assay with a large peer-sourced network of researchers, in tandem with the baseline dataset presented here, sets the scene for gauging ecosystem functioning at large scales to monitor impacts of global environmental change. In doing so, we address pressing needs for effective process-based tools (25) that can be deployed at large scales (6) by emerging international assessment programs (e.g., Intergovernmental Science-Policy Platform on Biodiversity and Ecosystem Services and Intergovernmental Panel on Climate Change) (7).

MATERIALS AND METHODS

Experimental approach

Our coordinated experiment used a peer-sourcing approach whereby each of approximately 150 research teams distributed worldwide de-

ployed a standardized assay in four rivers and their adjacent riparian zones. With this approach, we retrieved samples from 514 rivers and 533 riparian zones (1047 sites in total). Despite the unprecedented global coverage of our field experiment, gaps in spatial coverage exist as a result of a lack of available researchers in some areas (e.g., the Siberian steppe) or scarcity of flowing water ecosystems (e.g., Saharan Africa). Partners were drawn from professional relationships and research networks and by responses to invitations posted on the websites of professional organizations (e.g., the Society for Freshwater Science and Ecological Society of America). Each researcher was sent a kit that contained experimental materials, along with a detailed field and laboratory protocol. The distributed cotton strips were incubated in the field for approximately 4 weeks during 2015 and 2016 and shipped to the Aquatic Ecology Laboratory at Oakland University for analysis.

Decomposition assay

The cotton strip assay was chosen because the strips are composed of greater than 95% cellulose—the most abundant polymer on Earth and the main constituent of terrestrially derived leaf litter (15)—and because the assay is readily standardized (9). Such standardization is essential because failure to standardize so blurs large-scale patterns in the capacity of rivers and riparian zones to process organic carbon. For example, among the 2182 studies related to decomposition in riverine ecosystems published since 2000, only a handful have rates that are truly comparable (fig. S1). Even within studies, the attribution of differences in carbon processing rate to variation in environmental conditions is questionable because of the confounding effects that arise from variation in litter quality across space. This is inherently problematic at large spatial scales where there is growing appreciation of variation in leaf traits (16), including riparian litter (18). By using an identical cotton strip assay across all sites, we provide information on the capacity of ecosystems to process organic carbon. Additional reasons for using this assay are its sensitivity to environmental conditions, including temperature and nutrient availability (26), ease of use, suitability for both terrestrial and aquatic habitats, and the fact that dry samples can be readily shipped.

A trade-off of using any standardized organic matter in studies that span large spatial scales is that the quality of the standard organic matter will differ from natural inputs because their quality varies across large scales (18). In addition, because the quantity of organic matter inputs also varies spatially, decomposition assays do not necessarily reflect the quantity of organic matter that is being decomposed. Rather, the cotton strip assay and others (e.g., litter bag assays) are designed to quantify the relative capacity of ecosystems to decompose organic matter (i.e., decomposition potential) (10). Another trade-off is that the cotton strip assay isolates the activity of microbial heterotrophs and does not directly account for decomposition from the feeding activity of invertebrates (9).

The cotton strip assay relies on quantifying tensile strength loss of the cotton fabric, a process that reflects the microbial catabolism of cellulose (9, 10). Individual cotton strips (8.0 cm by 2.5 cm) were prepared from bolts of 12-ounce, heavy-weight cotton fabric (Style 548; Fredrix, Lawrenceville, GA, USA) and were each 28 threads in width (9). Strips were shipped to each partner along with reference strips that were not incubated in the field to obtain estimates of the initial tensile strength and to detect any changes occurring during shipping. Tensile strength was determined by placing each cotton strip in the jaws of a Mark-10 MG100 tensiometer mounted to a motorized test stand and pulling

them at a rate of 2 cm/min (9) until the strips tore. The maximum tensile strength (T_{MAX}) for each strip was recorded (in units of mass) and used for subsequent calculations. Individual T_{MAX} values from control and incubated strips were used in a hierarchical Bayesian model to calculate estimates of carbon processing rates (k).

Field methods

Each partner deployed the assay in four or more reference rivers (i.e., those characterized by minimal human impacts) and their adjacent riparian zones (i.e., the semi-aquatic terrestrial ecosystems immediately adjacent to permanent water bodies) during a time of the year when there were peak inputs of terrestrially derived organic matter (e.g., autumn leaf fall in temperate deciduous forests and the dry season in tropical dry forests). In each river, four replicate cotton strips were attached via cable binders and twine to stakes that were hammered into the river substrate of riffle or riffle-type habitats. This procedure was repeated in the riparian area adjacent to the river habitats where the cotton strips were deployed. In riparian zones, cotton strips were placed on the soil surface to simulate organic-matter input by senescent leaves. The cotton strips were distributed evenly between two locations in each habitat (i.e., each site) (2 cotton strips per location, 2 locations per habitat, 2 habitats, 4 rivers/riparian zones, and 32 cotton strips total per partner) that were separated by a distance of approximately five to seven bankfull channel widths. The strips were removed after approximately 3 to 4 weeks, an amount of time that was estimated to result in approximately 50% tensile strength loss; this degree of decomposition is believed to maximize the sensitivity of the assay to variation in environmental conditions (9).

Temperature data and Geographic Information System

In most instances, a temperature logger was placed in each river and each riparian zone and programmed to record hourly. This protocol yielded temperature data for 352 river and 343 riparian sites. Data from each logger were explored using a Python-based tool that facilitated data preprocessing tasks such as enforcement of a common date format, ensuring that all temperature readings were in centigrade, and transfer and consolidation of raw temperature readings from hundreds of files into a single database. The statistical computing package R was used to develop scripts for data processing, summarization, and plotting. Temperature readings for periods in which the logger was out of the water were removed, as were readings associated with obvious logger malfunctions. Plots and summary statistics were reviewed to confirm that remaining temperature readings were valid. Degree days were computed using positive temperature readings to generate daily mean temperatures and summing them.

Geographic Information System (GIS) and latitude and longitude data were used to ascribe a biome to each field site using a modified classification scheme (27) that was downloaded from the Environmental Systems Research Institute (ESRI) map server. In a small number of instances, field sites were located near transitional areas between two biomes and were noted by project partners as possibly having an incorrect biome classification. For the sake of repeatability, the original GIS-based biome classification method was retained. Latitude and longitude were determined at each river-riparian pair by each project partner using GPS or geo-referenced satellite photographs. A spatial join was performed between the biome layer and that which displayed the geographical location of the field sites. Biomes that do not have rivers and riparian zones (e.g., lakes) were not included in analyses.

Statistical analyses

Decomposition rates (k) were estimated from river and riparian zones separately using a standard exponential decay function and a Bayesian hierarchical model

$$\begin{aligned} g(k_j, P_j, T^C) &= e^{-k_j \times P_j + T^C} \\ [k_j, \sigma, T^C, \sigma^C | P_j, y_{ij}, y_l^C] \\ &\propto \text{lognormal}(y_{ij} | \log(g(k_j, P_j, T^C)), \sigma) \times \text{lognormal}(y_l^C | T^C, \sigma^C) \\ &\times \text{lognormal}(k_j | -4.35, 2.09) \times \text{lognormal}(T^C | 4.2, 32) \\ &\times \text{uniform}(\sigma | 0, 100) \times \text{uniform}(\sigma^C | 0, 100) \end{aligned}$$

where y_{ij} is the natural log tensile strength measured on the i th replicate strip from the j th site, k_j is the site-specific decomposition rate (k_D , in units of 1/day), T^C is the natural log T_{MAX} of all the replicate incubated control strips (y_l^C), and P_j is the period of exposure in days. Because of the limited number of cotton strips at each site, individual error terms could not be modeled for each river or riparian habitat, but single pooled SD for incubated (σ) and control cotton strips (σ^C) provided adequate fits for all cotton strips. A similar model was used to calculate temperature-corrected decomposition rates (k_{DD} , 1/degree day), where the exposure period (P_j) was the mean daily temperature accumulated over the incubation period ($^{\circ}\text{C} > 0$) and the priors on k_j were $\alpha = -6.57$ and $\beta = 2.24$. Error terms were assigned relatively uninformative priors, but T^C and k were given informed priors. The prior for T^C was derived from data for control strips of the same material used in previous studies, and the inflated β was used to account for any potential handling damage that may have occurred in this unique study. For priors on k , we used a global synthesis of leaf litter breakdown (5) to place constraints on our expectations of decomposition rates (28). Decomposition rates were assumed to be distributed log-normally and were given mean natural log k_D and k_{DD} (α) that matched the values from the literature (5); however, the SD of natural log k_D and k_{DD} (β) was inflated (β prior = $\sigma \ln(k) \times 2$) to slightly reduce the information content of the prior (28), which was done to reflect potential differences in decomposition rates between litter and cotton strips. The ratio of decomposition rates in river and riparian habitats was calculated for each complete river-riparian pair. Bayesian models were implemented in JAGS using the R package rjags. Three parallel chains with different initial conditions were run, chains were evaluated for convergence and mixing, and posterior distributions from 10,000 samples were generated.

Decomposition rates from each river-riparian site combination were then used in subsequent analyses to assess patterns in decomposition across biome, latitude, and temperature. Estimates of mean (and 95% credible interval) decomposition rates and ratios of river-riparian rates were compared across biomes using a Bayesian implementation of linear models via the brms function in R. Similarly, linear regressions between k_D and the inverse relative temperature (normalized to 10 $^{\circ}\text{C}$) and k_{DD} and latitude were completed with the brms package. The slope of the relationship between temperature and $\ln(k_D)$ is activation energy (E_a), and values of E_a were contrasted between riparian- and river-incubated cotton strips by comparing the posterior distributions of those parameters. Variance explained (i.e., Bayesian R^2) by a factor (e.g., biomes) was calculated according to published procedures (29). All decomposition rates and river-riparian ratio values were log-transformed before fitting linear models. Standard decomposition rates (k_D) exhibited heterogeneous variance across latitudes, and so we used quantile regression to estimate relationships between k_D

Supplementary Materials. All data presented here and model code are available at <https://github.com/dmcostello/CELLEX2018>. Additional data related to this paper may be requested from the authors.

Submitted 8 August 2018

Accepted 29 November 2018

Published 9 January 2019

10.1126/sciadv.aav0486

Citation: S. D. Tiegs, D. M. Costello, M. W. Isken, G. Woodward, P. B. McIntyre, M. O. Gessner, E. Chauvet, N. A. Griffiths, A. S. Flecker, V. Acuña, R. Albariño, D. C. Allen, C. Alonso, P. Andino, C. Arango, J. Aroviita, M. V. M. Barbosa, L. A. Barmuta, C. V. Baxter, T. D. C. Bell, B. Bellinger, L. Boyero, L. E. Brown, A. Bruder, D. A. Bruesewitz, F. J. Burdon, M. Callisto, C. Canhoto, K. A. Capps, M. M. Castillo, J. Clapcott, F. Colas, C. Colón-Gaud, J. Cornut, V. Crespo-Pérez, W. F. Cross, J. M. Culp, M. Danger, O. Dangles, E. de Eyto, A. M. Derry, V. D. Villanueva, M. M. Douglas, A. Eloise, A. C. Encalada, S. Entekin, R. Espinosa, D. Ethaiya, V. Ferreira, C. Ferriol, K. M. Flanagan,

T. Fleituch, J. J. Follstad Shah, A. Frainer, N. Friberg, P. C. Frost, E. A. García, L. García Lago, P. E. García Soto, S. Ghatge, D. P. Gilling, A. Gilmer, J. F. Gonçalves Jr., R. K. Gonzales, M. A. S. Graça, M. Grace, H.-P. Grossart, F. Guérol, V. Gulis, L. U. Hepp, S. Higgins, T. Hishi, J. Huddart, J. Hudson, S. Imberger, C. Iñiguez-Armijos, T. Iwata, D. J. Janetski, E. Jennings, A. E. Kirkwood, A. A. Koning, S. Kosten, K. A. Kuehn, H. Laudon, P. R. Leavitt, A. L. Lemes da Silva, S. J. Leroux, C. J. LeRoy, P. J. Lisi, R. MacKenzie, A. M. Marcarelli, F. O. Masese, B. G. McKie, A. O. Medeiros, K. Meissner, M. Miliša, S. Mishra, Y. Miyake, A. Moerke, S. Mombrikotb, R. Mooney, T. Moulton, T. Muotka, J. N. Negishi, V. Neres-Lima, M. L. Nieminen, J. Nimptsch, J. Ondruch, R. Paavola, I. Pardo, C. J. Patrick, E. T. H. M. Peeters, J. Pozo, C. Pringle, A. Prussian, E. Quenta, A. Quesada, B. Reid, J. S. Richardson, A. Rigosi, J. Rincón, G. Rîșnoveanu, C. T. Robinson, L. Rodríguez-Gallego, T. V. Royer, J. A. Rusak, A. C. Santamans, G. B. Selmeçy, G. Simiyu, A. Skuja, J. Smykla, K. R. Sridhar, R. Sponseller, A. Stoler, C. M. Swan, D. Szlag, F. Teixeira-de Mello, J. D. Tonkin, S. Uusheimo, A. M. Veatch, S. Vilbaste, L. B. M. Vought, C.-P. Wang, J. R. Webster, P. B. Wilson, S. Woelfl, M. A. Xenopoulos, A. G. Yates, C. Yoshimura, C. M. Yule, Y. X. Zhang, J. A. Zwart, Global patterns and drivers of ecosystem functioning in rivers and riparian zones. *Sci. Adv.* **5**, eaav0486 (2019).

Global patterns and drivers of ecosystem functioning in rivers and riparian zones

Scott D. TiegsDavid M. CostelloMark W. IskenGuy WoodwardPeter B. McIntyreMark O. GessnerEric ChauvetNatalie A. GriffithsAlex S. FleckerVicenç AcuñaRicardo AlbariñoDaniel C. AllenCecilia AlonsoPatricio AndinoClay ArangoJukka AroviitaMarcus V. M. BarbosaLeon A. BarmutaColden V. BaxterThomas D. C. BellBrent BellingerLuz BoyeroLee E. BrownAndreas BruderDenise A. BruesewitzFrancis J. BurdonMarcos CallistoCristina CanhotoKrista A. CappsMaria M. CastilloJoanne ClapcottFanny ColasCheco Colón-GaudJulien CornutVerónica Crespo-PérezWyatt F. CrossJoseph M. CulpMichael DangerOlivier DanglesElvira de EytoAlison M. DerryVeronica Díaz VillanuevaMichael M. DouglasArturo ElosegíAndrea C. EncaladaSally EntekinRodrigo EspinosaDiana EthaiyaVerónica FerreiraCarmen FerriolKyla M. FlanaganTadeusz FleituchJennifer J. Follstad ShahAndré FrainerNikolai FribergPaul C. FrostErica A. GarciaLiliana García LagoPavel Ernesto García SotoSudeep GhateDarren P. GilingAlan GilmerJosé Francisco Gonçalves Jr.Rosario Karina GonzalesManuel A. S. GraçaMike GraceHans-Peter GrossartFrançois GuérolVlad GulisLuiz U. HeppScott HigginsTakuo HishiJoseph HuddartJohn HudsonSamantha ImbergerCarlos Iñiguez-ArmijosTomoya IwataDavid J. JanetskiEleanor JenningsAndrea E. KirkwoodAaron A. KoningSarian KostenKevin A. KuehnHjalmar LaudonPeter R. LeavittAurea L. Lemes da SilvaShawn J. LerouxCarri J. LeRoyPeter J. LisiRichard MacKenzieAmy M. MarcarelliFrank O. MaseseBrendan G. McKieAdriana Oliveira MedeirosKristian MeissnerMarko MilišaShailendra MishraYo MiyakeAshley MoerkeShorok MombrikotbRob MooneyTim MoultonTimo MuotkaJunjiro N. NegishiVinicius Neres-LimaMika L. NieminenJorge NimptschJakub OndruchRiku PaavolaSabel PardoChristopher J. PatrickEdwin T. H. M. PeetersJesus PozoCatherine PringleAaron PrussianEstefania QuentaAntonio QuesadaBrian ReidJohn S. RichardsonAnna RigosiJosé RincónGeta Rî#noveanuChristopher T. RobinsonLorena Rodríguez-GallegoTodd V. RoyerJames A. RusakAnna C. SantamansGéza B. SelmeczyGelas SimiyuAgnija SkujaJerzy SmyklaKandikere R. SridharRyan SponsellerAaron StolerChristopher M. SwanDavid SzlagFranco Teixeira-de MelloJonathan D. TonkinSari UusheimoAllison M. VeachSirje VilbasteLena B. M. VoughtChiao-Ping WangJackson R. WebsterPaul B. WilsonStefan WoelflMarguerite A. XenopoulosAdam G. YatesChihiro YoshimuraCatherine M. YuleYixin X. ZhangJacob A. Zwart

Sci. Adv., 5 (1), eaav0486. • DOI: 10.1126/sciadv.aav0486

View the article online

<https://www.science.org/doi/10.1126/sciadv.aav0486>

Permissions

<https://www.science.org/help/reprints-and-permissions>

Use of this article is subject to the [Terms of service](#)

Science Advances (ISSN 2375-2548) is published by the American Association for the Advancement of Science, 1200 New York Avenue NW, Washington, DC 20005. The title *Science Advances* is a registered trademark of AAAS.

Copyright © 2019 The Authors, some rights reserved; exclusive licensee American Association for the Advancement of Science. No claim to original U.S. Government Works. Distributed under a Creative Commons Attribution NonCommercial License 4.0 (CC BY-NC).